Chemical Papers
https://doi.org/10.1007/s11696-022-02392-w

ORIGINAL PAPER

Green synthesis and characterization of silver nanoparticles using *Morinda lucida* leaf extract and evaluation of its antioxidant and antimicrobial activity

Ayomide H. Labulo[1] · Oyinade A. David[2] · Augustine D. Terna[3]

Received: 18 May 2022 / Accepted: 22 July 2022

Abstract
This study emphasizes the production of eco-friendly silver nanoparticles from a medicinal plant extract of *Morinda lucida (M. lucida)* and investigated its antioxidant and antimicrobial activity. Phytochemical screening of *M. lucida (ML)* leave extract was carried out and observed to contain some fundamental phyto-reducing agents such as reducing sugar, proteins, and alkaloids. The green synthesized AgNPs (ML-AgNPs) were characterized by UV–vis spectroscopy, Fourier transform infrared spectroscopy (FTIR), transmission emission microscopy (TEM), scanning electron microscopy (SEM), X-ray diffraction (XRD), and Energy dispersive X-ray analysis (EDX). Thermo gravimetric analysis (TGA) was performed on the synthesized ML-capped AgNPs to determine the thermal stability and the formation of the green synthesized AgNPs. The formation of AgNPs was confirmed by the UV–vis absorption spectra, which showed an absorption band at 420 nm. The morphology of ML extract-mediated AgNPs was mostly spherical and rough-edged crystallite nanostructures, with an average particle size of 11 nm. The FTIR analyses revealed distinctive functional groups which were directly involved in the synthesis and stability of AgNPs. The crystallite size was 8.79 nm, with four intense peaks at 2θ angles of 38°, 44°, 64°, and 77°. At an energy level of 3.4 keV, a significant signal was observed indicating the production of thermally stable and pure crystallite AgNPs. The antioxidant property of green synthesized ML-AgNPs was determined to be 40% higher than that of crude *M. lucida* leaf extract. The ability of green synthesized ML-AgNPs to scavenge free radicals also increased in the order of $OH^- < NO < H_2O_2$. The ML-AgNPs have strong activities with a maximum against *P. vulgaris* and a minimum with *E. faecalis.*

Keywords *Morinda lucida* · Green synthesis · Silver nanoparticles · Antioxidant · Antimicrobial activity

Introduction

Nanoscience is a fascinating branch of science concerned with the use and development of structures and materials with nanometer-scale dimensions. Nanotechnology advancements have benefited scientists in their search for a novel approach to manufacturing nanomaterials for antimicrobials (Naikoo et al. 2021), agricultural production (Ndlovu et al. 2020), engineering (Dhanapal 2012), and catalysis (Wu et al. 2020; Li et al. 2021; Xu et al. 2021). Nanoparticles (NPs) are small particles with a diameter of 1–100 nm that can be made in a variety of ways. When compared to bulk materials, NPs are articles with different physical, thermal, and chemical properties (Khan et al. 2019). NPs can be synthesized using various methods, but some involved the use of hazardous and poisonous substances that provide a high risk of toxicity (Khan et al. 2019). Green synthesis is one of the most environmentally friendly and low-cost approaches with high reproducibility and yield (Hano and Abbasi 2022). Apart from the use of bacteria, fungi, and algae, aqueous extracts of leaves have been found to reduce silver salt and instantly capped the nanosized silver to reduce agglomeration (Ansar et al. 2020). Metal nanoparticles, such as silver nanoparticles (AgNPs), are appealing due to their diverse

✉ Ayomide H. Labulo
ayomide.labulo@science.fulafia.edu.ng

[1] Department of Chemistry, Federal University of Lafia, Lafia, Nasarawa State, Nigeria

[2] Department of Plant Science and Biotechnology, Federal University Oye-Ekiti, Oye-Ekiti, Ekiti State, Nigeria

[3] Department of Chemistry, Federal University of Technology, PMB 1526, Owerri, Imo State, Nigeria

Published online: 16 August 2022

applications in pharmaceuticals (Contreras 2012), including the treatment of acne and dermatitis, as well as post-surgical infection (Contreras 2012). Silver, among other metals, has been proven to be more hazardous to microbes while being less toxic to mammalian cells (Verma and Stellacci 2010). AgNPs have found widespread application in the design of multi-resistant medications (Ojemaye et al. 2021) because of their unusual stability, diverse geometries, and ease of release of silver to impede the growth of bacterial cells by creating reactive hydrogen peroxide. Water treatment (Zhao et al. 2021), agriculture (Khan et al. 2021), biomedical (Akintelu et al. 2021), catalysis (Ajitha et al. 2021), and sensing (Jiang et al. 2022) are only a few other applications of AgNPs that have been reported. In this study, AgNPs were synthesized from the extract of the brimstone tree (*M. lucida*), a medium-sized tree with crooked, short branches. *M. lucida* plant can be commonly found in Senegal, Nigeria, Sudan, Angola, and Zambia (Agyare et al. 2013). It is sometimes planted around villages, e.g., in Benin (Tran et al. 2013). In Nigeria, the stem is popular as a chewing stick (Agyare et al. 2013). The root, bark, and leaves decoctions and infusions are used as remedies against malaria, diabetes, stomach aches, ulcer, leprosy, and different type of fever (Abbiw 1990). *M. lucida* has been found to contain high content of alkaloids, flavonoids, anthraquinones, and phytochemicals which are good anti-carcinogenic, anti-inflammatory, and antioxidants (Feng et al. 2018). *M. lucida* was investigated for the first time in this study for the synthesis of AgNPs. The synthesized ML-AgNPs were characterized and we investigated the total antioxidant potency of the aqueous extract of *M. lucida* and the green synthesized ML-AgNPs.

Materials and methods

Collection of plant materials and chemical reagents

The medicinal plants used for this study were collected in February 2020 around Ibadan metropolis, Oyo state Nigeria Latitude 7.3775° N, and Longitude 3.9470° E. The herbal plant was identified as *M. lucida* (Brimstone) (Fig. 1) also known as *Oruwo* in the Yoruba language and was brought to the laboratory for preparation. The plant leaves were identified as *Morinda lucida* at the herbarium of the Department of Botany and Plant Science, Federal University of Lafia. Silver nitrate ($AgNO_3$ 99.80%) was supplied by Sigma-Aldrich Chemicals (South Africa).

Preparation of *M. lucida* leaf aqueous extract

Plant leaves were thoroughly cleaned with distilled water before being dried in the open air. After the leaves had completely dried, they were pulverized with a porcelain mortar and pestle, and the samples were stored in well-labeled air-tight plastic containers (Labulo et al. 2015). 10 g of aqueous leaf extracts were weighed and boiled in 600 mL of deionized water at 100 °C for 20–30 min. The extract was then filtered through Whatman 185 m filter paper, yielding a light brown colored filtrate (Fig. 2). The extract was kept in the refrigerator between 4 and 10 °C for 10–15 days and utilized for the synthesis of AgNPs.

Phytochemicals screening

Phytochemical screening was carried out using the plant extracts to determine the presence of the following compounds: phenols and tannins, saponins, triterpenes, flavonoids, alkaloids, and steroids according to the procedure outlined by Hedge et al. (2010).

Fig. 1 Images of the leaves of *M. lucida*

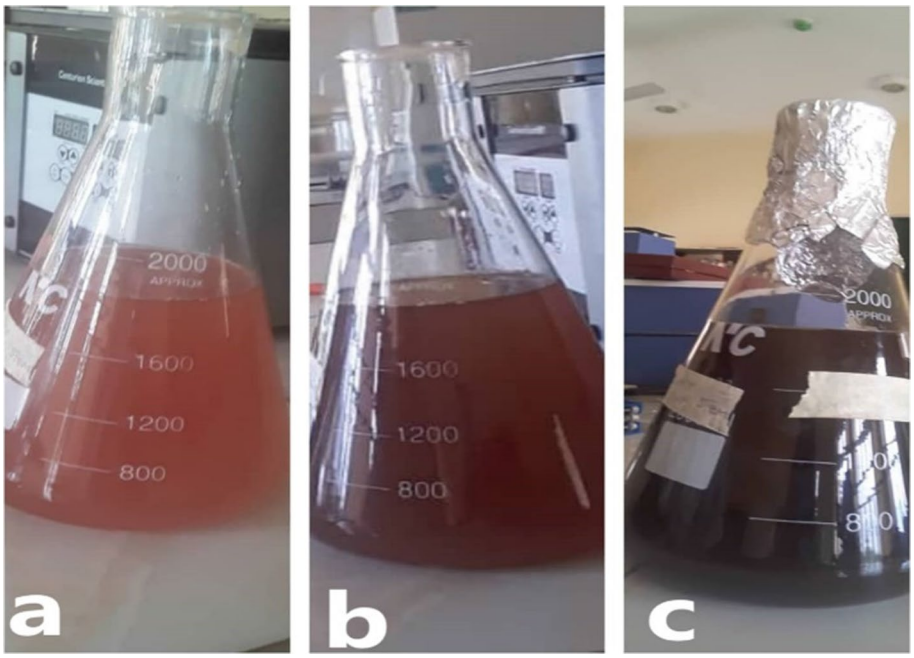

Fig. 2 **a** *M. lucida* plant extract **b** *M. lucida* plant extract and silver nitrate after 2 h **c** *M. lucida*-silver nanoparticles (ML-AgNPs) after 24 h of incubation

Test for phenols and tannins

A few drops of 3% $FeCl_3$ were added to a 1 mL solution of the extract and shaken a little. The presence of phenolic compounds and tannins was detected by the appearance of a deep blue coloration formed.

Test for saponins

A portion of the extract solution for both plants was put in two different clean test tubes and shaken vigorously, then left for a few minutes. The presence of saponins was detected by the formation of a stable froth in the solution.

Test for triterpenes

1 mL of chloroform was added to the extract solutions and reacted with 1 mL of conc. H_2SO_4 by carefully sliding it down the walls of the test tubes containing the solutions. The presence of Triterpenes was confirmed by the formation of red coloration in the solution.

Test for flavonoids

Lead acetate solution was added to 1 mL of the extract solutions and the presence of flavonoids was confirmed by the formation of a yellow precipitate in the solution.

Test for alkaloids

The alkaloid test was carried out by adding 5 mL of HCl to the extract solution. The solution was agitated, filtered, and kept for further analysis. Meyer's test was done afterward by adding 2 mL of the filtrate to 5 mL of Meyer's reagent. The formation of a yellow precipitate indicates the presence of alkaloids.

Test for steroids

2 mL of the extract solution was mixed with 1 mL of acetic anhydride and heated for a few minutes then cooled. Few drops of conc. H_2SO_4 was added by sliding it down the side of the test tube containing the solution. The presence of steroids was indicated by the appearance of a blue coloration.

Synthesis of silver nanoparticles from plant extracts

The synthesis of silver (Ag) nanoparticles was carried out according to the method described by Dada et al. (2015). In a typical experiment, 10 mL of the aqueous leaf extract was measured and placed into a clean 250 mL beaker, where it was reacted with 40 mL of 1 mM $AgNO_3$ at room temperature (Fig. 3). The synthesized mixture was allowed to stand for 24 h before being separated by centrifugation at 4000 rpm for 30 min. The transparent liquid was decanted, and the settling layer (i.e., nanoparticles) was dried in the

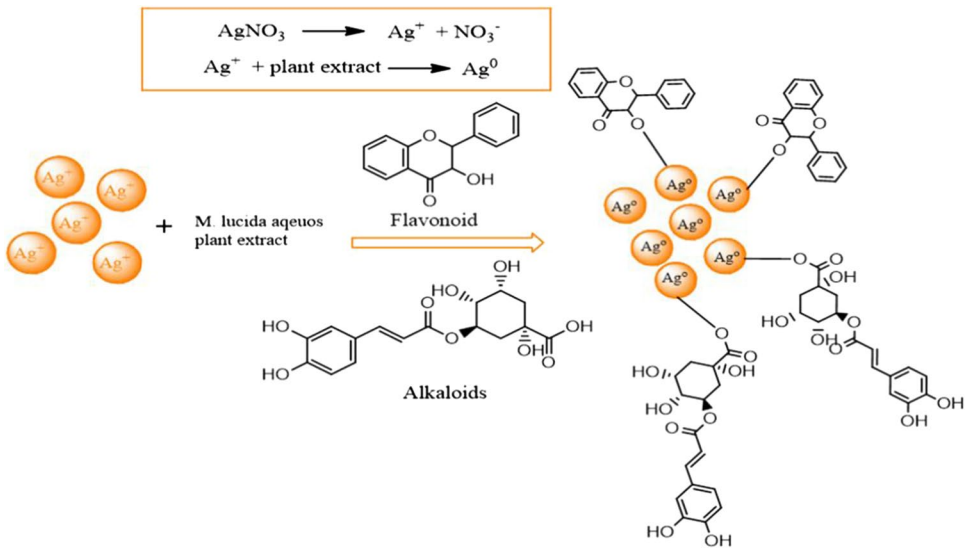

Fig. 3 Proposed schematic diagram of the reduction mechanism of silver nitrate by the aqueous leaf extract of *M. lucida*

oven at 30 °C and stored in a 5 mL plastic sample vial with the appropriate labeling. The NPs formed were labeled as the *M. lucida*-silver nanoparticles (ML-AgNPs).

Characterization

The Biochrom Libra PCB 1500 UV–vis spectrophotometer was used to measure the absorbance of the green-produced AgNPs. The absorbance of silver nanoparticles dispersed in a quartz cuvette with a 1 cm optical path was measured by removing a small aliquot from the reaction mixture. The intrinsic characteristics of the formed AgNPs were investigated using energy dispersive X-ray (EDX), X-ray diffraction (XRD), scanning electron microscopy (SEM), transmission electron microscopy (TEM), Fourier-transform infrared spectroscopy (FTIR), and thermogravimetric analysis (TGA). The approximate sizes and shapes of AgNPs were examined using SEM (TESCAN Vega TS 5136LM SEM typically at 20 kV at a working distance of 20 nm) and TEM by dropping an aqueous solution containing the silver nanoparticles onto the carbon-coated grids and drying under an infrared lamp. Micrographs were obtained using a Philips Morgagni (M-268) operating at 80 kV. XRD analysis was done by model D8 ADVANCE apparatus (Bruker, USA), and FTIR analysis was performed using a SHIMADZU FTIR model IR8400s spectrophotometer, which provided information on functional groups and biomolecules present on the surface of AgNPs during their formation. Thermogravimetric analyses for thermal stability of the AgNPs were performed using TA instrument Q series™ thermal analyzer DSC/TGA (Q600). XRD pattern was recorded using a graphite monochromatized high-density Cu Kα radiation ($\lambda = 0.15406$ Å) by Rigaku/Dmax RB.

Anti-oxidant property

Cupric reducing antioxidant capacity (CUPRAC) assay

The CUPRAC assay method was utilized with slight adjustments to evaluate the cupric ions (Cu^{2+}) reduction ability of the extracts, as described by Gulcin et al. (2004). In a test tube, 0.25 mL $CuCl_2$ solution (0.01 M), 0.25 mL ethanolic neocuproine solution (7.5×10^{-3} M), and 0.25 mL acetate buffer (1 M) were mixed altogether, then 0.25 mL extracts were mixed. With distilled water, the total reaction volume was set at 2 mL, and the solution was thoroughly mixed. The tubes were sealed and maintained at room temperature for 30 min before being tested for absorbance at 450 nm. Increased absorbance indicates greater reduction potential, which is represented as Trolox equivalent (TEAC) when Trolox is used as the standard.

Ferrous ion-chelating ability assay The ferrous ion chelating (FIC) assay was performed using Singh and Rajini method (Singh and Rajini 2004), with significant modifications. 2 mM $FeCl_2 \cdot 4H_2O$ and 5 mM ferrozine solutions were diluted 20 times. In a nutshell, an aliquot (1 mL) of various extract strengths was combined with 1 mL $FeCl_2 \cdot 0.4H_2O$. The reaction was started by adding ferrozine after 5 min of incubation (1 mL). The mixture was vigorously shaken, and the absorbance of the solution was measured spectrophotometrically at 562 nm after another 10 min of incubation.

The percentage inhibition of ferrozine—Fe^{2+} complex formation was calculated by using the formula:

$$\%\,\text{Chelating effect} = \left[\left(A_{\text{control}} - A_{\text{sample}}\right)/A_{\text{control}}\right] \times 100 \quad (1)$$

where, $A_{control}$ = absorbance of the control sample (the control contains $FeCl_2$ and ferrozine, complex formation molecules) and A_{sample} = absorbance of tested samples.

Reductive potential

The reductive potential of the extract was determined according to the method of Oyaizu (1986) and as described by Gulcin et al. (2004). The extracts (1 mL) were mixed with 1 mL of phosphate buffer (pH 6.6, 0.2 M) and refluxed before adding 2.5 mL of 1% potassium ferricyanide. The reaction mixture was then incubated for 20 min in a water bath at 50 °C. The mixture was then treated with 2.5 mL of 10% trichloroacetic acid and centrifuged for 10 min. The mixture was vortexed after adding 2.5 mL (100 L) of supernatant, 2.5 mL (distilled water), and 0.5 mL (20 L) of 0.1% ferric chloride. At 700 nm, the absorbance was measured. The reaction mixture's higher absorbance suggests a stronger reductive potential.

The reductive potential was expressed as a reductive potential index (REI) as shown below;

$$\text{REI} = \text{Absorbance of extract} \,/\text{Absorbance of 10 } \mu\text{g/mL vitamin C standard} \quad (2)$$

Assay of hydroxyl radical scavenging activity (OH^-)

According to the method of Halliwell et al. (1987), the hydroxyl radical scavenging activity was assessed by evaluating the competition between deoxyribose and the fractions for hydroxyl radicals generated from the Fe^{3+}/ascorbate/EDTA/H_2O_2 system. Reaction mixture of 1.0 mL reagent composed of 3.0 mM deoxyribose, 0.1 mM EDTA, 2 mM H_2O_2, 0.1 mM L-Ascorbic acid, 0.1 mM $FeCl_3 \cdot 6H_2O$ in 10 mM phosphate buffer, pH 7.4 were prepared and various fraction concentrations (50–350 g/mL) were added to the reaction mixture. After 1 h of incubation at 37 °C, 1.0 mL of 1% (w/v) TBA (in 0.25 N HCl) and 1.0 mL of 10% (w/v) TCA were added to the reaction solutions. The reaction mixtures were heated in a boiling water bath for 20 min at 100 °C, and the pink chromogen (malondialdehyde-(TBA) adduct) was extracted into 1.0 mL of butan-1-ol, with the absorbance measured at 532 nm against a blank solution.

The percentage inhibition was calculated using the expression:

$$\text{Percentage \% inhibition} = \left(\text{Abs}_{(\text{control})} - \text{Abs}_{(\text{sample})}\right)/\text{Abs}_{(\text{control})} \times 100 \quad (3)$$

Inhibition of nitric oxide radical (NO)

The extracts were tested for their ability to inhibit nitric oxide radical activity using the Green et al. method (Green et al. 1982), as reported by Marcocci et al. (Marcocci et al. 1994). Nitric oxide is produced when sodium nitroprusside in an aqueous solution at physiological pH reacts with oxygen to form nitrite ions, which may be quantified using the Griess reaction. The reaction mixture, which included 0.1 mL of oil extract at various concentrations (10, 5, 2.5, 1.25, 0.625, 0.3125 mg/mL) and 0.9 mL of sodium nitroprusside (2.5 mM) in phosphate buffer saline, was incubated for 150 min under illumination. Following incubation, 0.5 mL of 1% sulphanilamide in 5% phosphoric acid was added and incubated in the dark for 10 min, followed by 0.5 mL 0.1% NED (N-1-naphthyl ethylenediamine dihydrochloride) (Marcocci et al. 1994).

Scavenging of hydrogen peroxide (H_2O_2)

In phosphate-buffered (PBS) saline, a solution of hydrogen peroxide (20 mM) was prepared at pH 7.4. 1 mL extracts or standards in methanol were added to 2 mL hydrogen peroxide solutions in PBS at various concentrations. After 10 min, the absorbance was measured at 230 nm in comparison with a blank solution containing extracts in PBS without hydrogen peroxide (Jayaprakasha et al. 2004).

Antibacterial activity

Antimicrobial sensitivity

The antibacterial potency of ML-AgNPs and plant extract was assessed against Citrobacter, *E. coli*, *P. vulgaris*, *S. typhi*, *V. cholerae,* and *E. faecalis* using the disk diffusion method (Green et al. 1982). The prepared Whatman filter paper No.1 discs were soaked in ML-AgNPs and plant extract solutions and air-dried in a sterile environment. Agar plates were prepared by swabbing the bacteria cultures uniformly unto individual plates. The plates were divided into four and placed upon the earlier prepared discs, then plates were incubated at 37 °C for 1–2 days and the zone of inhibition was measured by an ordinary scale (Khanom et al. 2018).

Results and discussion

Phytochemical compounds in the plant extract

Table 1 summarizes the phytochemical components found in the plant extract. Aqueous leaves extract of *M. lucida* contained alkaloids, flavonoids, tannins, terpenoids, anthraquinones, phlobatanin, carbohydrates, saponins, proteins, amino acids, and phytosterols while steroids, cardiac

Table 1 Qualitative analysis of the aqueous extracts of *M. lucida* leaf

Phytochemicals	Presence/Absence
Alkaloids	+
Steroids	–
Flavonoids	+
Tannins	+
Terpenoids	+
Anthraquinone	+
Phlobatanins	+
Cardiac glycosides	–
Reducing sugars	–
Carbohydrates	+
Saponins	+
Coumarin	–
Protein	+
Phenols	–
Amino acids	+
Phytosterols	+

+ present, – absent

glycosides, reducing sugars, coumarin, and phenols were absent. According to Gutorova et al. (2021), the presence of both alkaloids and flavonoids aids in the reduction in silver ions to generate AgNPs. Flavonoids were also found in green synthesized nanoparticles made from corn silk aqueous extract, according to Li et al. (2020). Previous phytochemical screening on *M. lucida* revealed that phenols, flavonoids, and reducing sugars are the major components of plants that have reducing power (Medina-Cruz et al. 2020). Therefore, as a result of the presence of both proteins and alkaloids in the *M. lucida* extract used in this study, the green-produced AgNPs should have high antioxidant potency.

UV–visible spectroscopy

The reduction in Ag^+ to Ag^0 was confirmed by a color change from light brown to a deep brown, indicating the formation of nanosilver (Fig. 2a–c). This was further confirmed using UV–vis spectrophotometer. The surface plasmon resonance (SPR) was observed for ML-AgNPs, with a band peak at 420 nm absorption maxima (Fig. 4a). A yield of 56% was calculated after centrifuging at 6000 rpm. According to Aref and Salem (2020), silver nanoparticles produced from *Cinnamomum camphora* had a wavelength of 420 nm. Hamelian et al. (2018) also found a strong and single peak in the UV–vis spectrum of colloidal AgNPs synthesized from *Thymus Kotschyanus* extract. In a study conducted by Aldosary and Abd El-Rahman (2019), an absorbance peak of 427–437 nm was identified for *C. sinensis* extract-AgNPs. Phenols, steroids, flavonoids, tannins, steroids, and saponins are among the metabolites found in *M. lucida* aqueous leaf extract that can reduce Ag^+ ions. The presence of flavonoids and protein in *M. lucida* aqueous extract can be linked to the plant extracts' ability to serve as a stabilizing and capping agent.

Total phenolic compounds

The secondary metabolites present in green plants such as phenolic compounds are essential for the reduction in metal ions into their corresponding nanosized metals (Konappa et al. 2021). The concentration of the metabolites can influence the yield, morphology, and particle size of the NPs. In Fig. 4b, it was observed that the total phenolic compounds in the extract and the AgNPs increase, with increased concentration. The leaf extract shows a phenolic content of about 18 µg/mL at the highest concentration of 160 µg/mL, while AgNPs showed a total phenolic content of 10 µg/mL at a

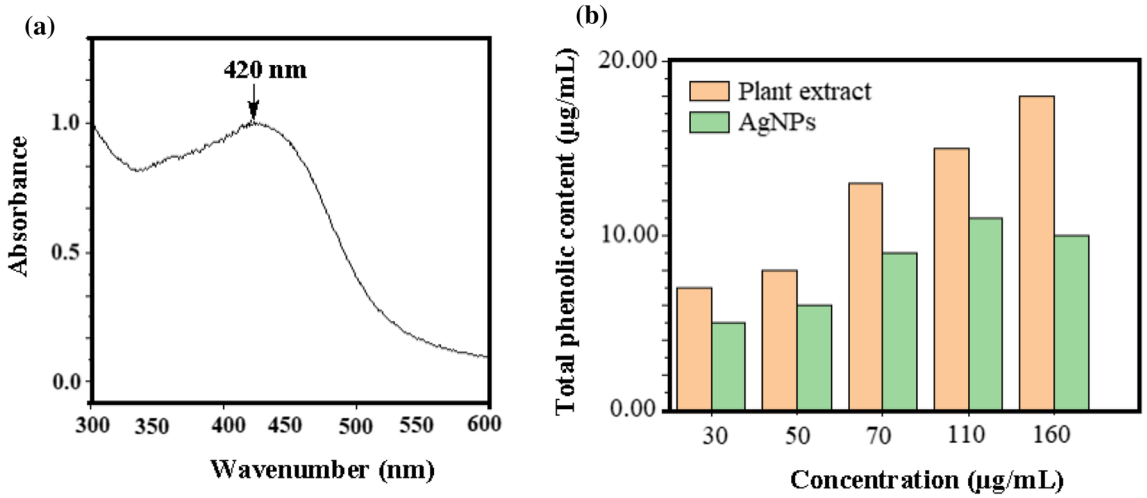

Fig. 4 **a** UV–visible spectra of green synthesized ML-AgNPs and **b** concentration of total phenolic compounds

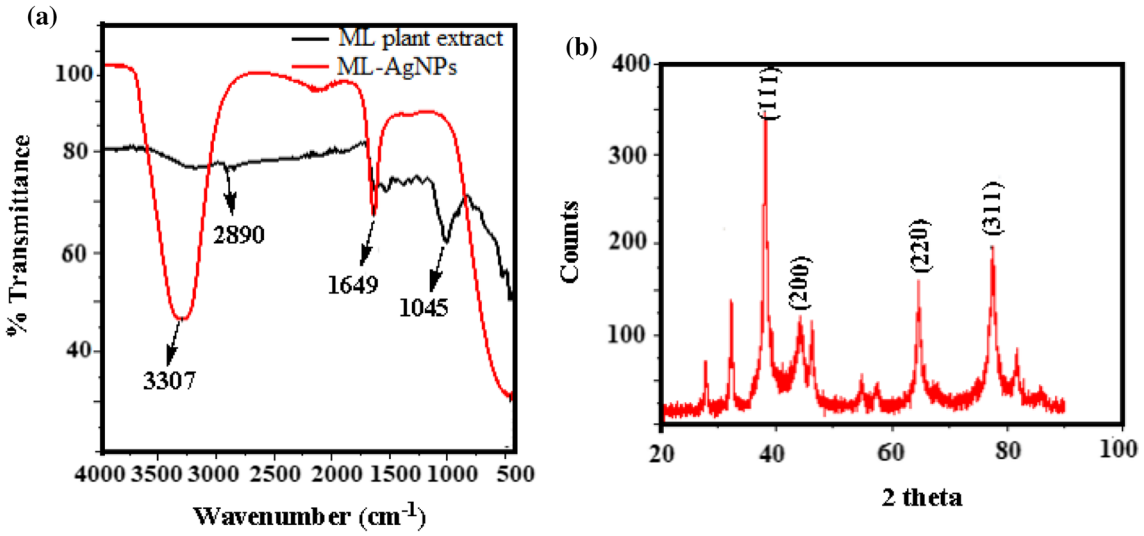

Fig. 5 **a** FTIR spectra of *M. lucida* plant extract and ML-AgNPs **b** XRD spectra of ML-AgNPs

similar concentration. This confirms that not all the metabolites and the antioxidant compounds are used up for the reduction in the Ag salt, but also act as the capping agent (Shoor and Lodise 2006).

FTIR analysis

The functional groups involved in capping and stabilizing the Ag nanoparticles were identified using FTIR between 4000 and 400 cm^{-1}. Figure 5a shows the spectra of the aqueous extract of *M. lucida* and ML-AgNPs. The aqueous extract of *M. lucida* showed characteristic peaks at 3307, 2890, and 1649 cm^{-1} which could be attributed to hydroxyl group O–H stretching (Labulo et al. 2015), C–H stretching vibrations of methyl, methylene, or methoxy groups, and C–O stretching in the carbonyl group (Shoor and Lodise 2006), and the N–H group of amines (Kumar et al. 2019), respectively. The broadband peak at 3307 cm^{-1} observed in the ML-AgNPs spectra could be attributed to the overlapping stretching mode of N–H and O–H functional groups (Kumar et al. 2019).

The C–O band at 1045 cm^{-1} may be assigned to the polyols (i.e., flavones, terpenoids, and carbohydrates) present in the plant extract. The various assignments are consistent with those published in the literature for related compounds (Medina-Cruz et al. 2020; Aref and Salem 2020; Gutorova et al. 2021). These organic compounds were identified as stabilizing groups and capping agents that contributed to the silver ions reduction to metallic silver. FTIR measurements indicated peaks corresponding to different functional groups such as carboxylic acids, alcohol, phenol, esters, ethers, aldehydes, alkanes, and proteins, which were involved in the synthesis and stabilization of AgNPs. Comparing the two spectra, C–O was observed in the ML-AgNPs spectra (Fig. 5a), implying that the system's stabilization was caused by the carbonyl group of the reducing sugars adhering to the silver (Ag) (Singh et al. 2013).

XRD

The XRD pattern of ML-AgNPs is shown in Fig. 5b. XRD pattern reveals four intense peaks at 38°, 44°, 64°, and 77°, which correspond to the face cubic centre (fcc) 111, 200, 220, and 311 planes of AgNPs, respectively. The results are consistent with those of Rahimi-nasrabadi et al. (2014). The other peaks in the spectra could be attributed to metabolite capping the AgNPs.

The size of the AgNPs was calculated by the Debye–Scherrer equation as follows:

$$D = \frac{k\lambda}{\beta \cos\theta} \tag{4}$$

where D is the crystallite size of the AgNPs, λ is the wavelength of the X-ray source (1.54056 Å), β is full width at half maximum (FWHM) of the diffraction peak in radian, k is the Scherrer constant that varies from 0.9 to 1, and θ is the Bragg angle in radian (Raja et al. 2017). The XRD pattern analysis of *ML*-AgNPs gave a crystallite size of the nanoparticles was 8.79 nm.

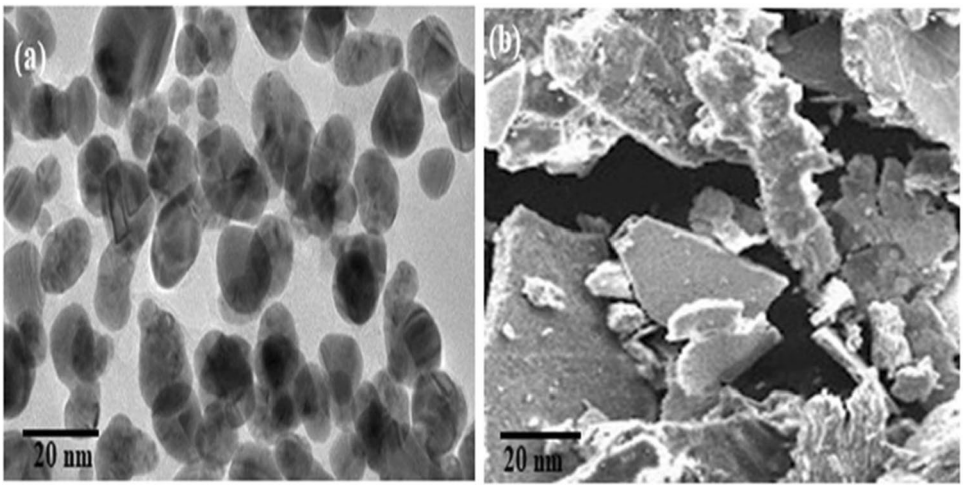

Fig. 6 **a** TEM and **b** SEM images of ML-AgNPs

TEM

TEM is a powerful tool in determining the morphologies, shapes, and sizes of metal NPs. The TEM image of ML-AgNPs shows the polydispersed-capped NPs (Fig. 6a). The obtained NPs are spherical with particle average particle size of 11 nm (Fig. 7a) similar to the findings of Zangeneh et al. (2019). It could be observed that the NPs are evenly distributed without agglomeration with transparent capped edges. This could be a result of the presence of phytosterol and amino acids from the *M. lucida* aqueous extract. The SEM image (Fig. 6b) shows a flake-like surface morphology of the ML-AgNPs.

EDX

Figure 7b shows the elemental composition of ML-AgNPs. The synthesized nanosilver showed a strong signal at 3.4 keV, with weak signals from N, O, C, Si, P, and Cl. The pure crystalline character of the ML-AgNPs was completely composed of silver, as indicated by the predominant emission energy at 3.4 keV. The findings of Matin et al. (Matin et al. 2017) on silver nanoparticles synthesized from *Peganum harmala* plant extract via the green approach are consistent with the findings in this work. Palani et al. (2015) reported a similar result utilizing synthetic melanoidin bacterial extracts and a 3.3 keV energy level for green manufactured AgNPs.

Thermo-gravimetric analysis (TGA)

The TGA plot of ML-AgNPs is shown in Fig. 8. TGA was carried out to determine the thermal stability and presence of oxygen functionality on the capped green synthesized ML-AgNPs (Nityanada and Kaushik 2012). TGA thermogram of the AgNPs showed three identical and continuous weight loss

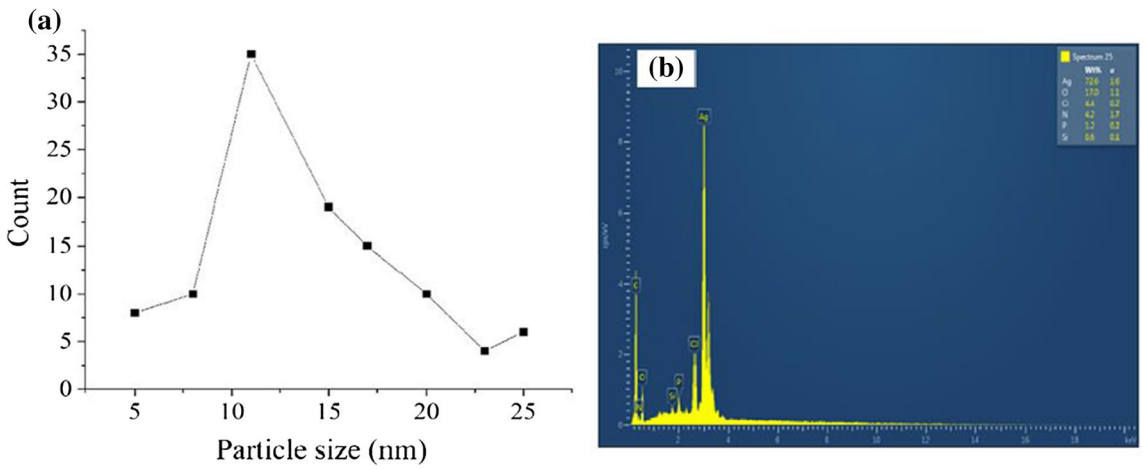

Fig. 7 **a** Particle size distribution **b** EDX spectra of ML-AgNPs

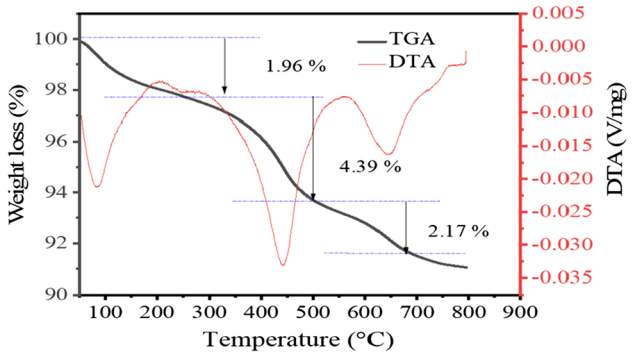

Fig. 8 TGA and DTA thermograms of ML-AgNPs

of stages (Fig. 10). The first decomposition stage occurs from room temperature to 160 °C with 1.96% weight loss indicating the removal of water containing impurities in the ML-AgNPs. The second stage was observed between the temperatures 160–559 °C with 4.39% weight loss, attributed to the decomposition of the capping organic compounds (such as carbonyl and the reducing sugar) agents acting as the core–shell. This result is in agreement with the result obtained from FTIR spectra (Fig. 5a). The third and final step is attributed to the decomposition of ML-AgNPs at elevated temperatures between 560 and 800 °C with a weight loss of 2.17%. The percentage purity of the green synthesized ML-AgNPs is estimated to be 91.48% pure silver. For a one-pot crystalline AgNPs synthesis, Nityananda and Kaushik (2012) reported a similar range of TGA.

Antioxidant property

Antioxidant, metal chelating, and free radical scavenging abilities of *M. lucida* extract and ML-AgNPs

The approaches used to measure antioxidant capacity include an electron transfer mechanism (Flieger et al. 2021), which includes a copper antioxidant capacity reduction test (CUPRAC). ML-AgNPs had a total antioxidant capacity that was 40% higher than the crude *M. lucida* extract (Table 2). The CUPRAC and reducing potential of the ML-AgNPs was two folds greater than the *M. lucida* extract (Table 2). The antioxidant property of green synthesized AgNPs as a result of the plant extract being a natural antioxidant material, hence, acted as a reducing and stabilizing agent in the green synthesis, resulting in the surface modification of AgNPs. The larger surface-area-to-volume ratio of ML-AgNPs, which enhances their reactivity towards radicals, can be attributed to the increased antioxidant activity of ML-AgNPs. Furthermore, the antioxidant mechanism of the plant-mediated silver nanoparticles, ML-AgNPs, can be attributed to the preferential sorption of extract components on the surface of the silver nanoparticles, AgNPs (Patil Shriniwas et al. 2017; Khandel et al. 2018). The result obtained is similar to the antioxidant property of *L. betulina*-capped AgNPs (Sytu and Camacho 2018). Previous studies have shown that the level of antioxidant capacity is dependent on the plant species and the botanical family (Ranjitham et al. 2013).

ML-AgNPs inhibited 75–90% hydrogen peroxide from concentrations ranged from 0.25 to 1.0 mg/l while *M. lucida* extract inhibited 50–68% H_2O_2. The ML-AgNPs had no significant inhibitory effect on Hydroxyl ions (OH^-) whereas, 0.25–1.0 mg/l. ML-AgNPs scavenged 50–60% Nitric oxide (NO) compared to the *M. lucida* extract. Thus the inhibitory factor of ML-NPs increased along with concentration. As a result, the average inhibitory capacity (IC_{50}) of ML-AgNPs improved as concentrations increased. The ability of ML-AgNPs to scavenge free radicals increased in the order $OH^- < NO < H_2O_2$ (Table 3). The IC_{50} values required to scavenge NO, OH–, and H_2O_2 were lower in ML-AgNPs compared to the *M. lucida* extract, implying that only small amounts of ML-AgNPs are required to scavenge the free radicals, further confirming better antioxidant properties than *M. lucida* extract (Fig. 9). The increased antioxidant activity of ML-AgNPs relative to the raw extract is intriguing since antioxidants protect humans from oxidative stress-related illnesses through chemoprotection (Ulewicz-Magulska and Wesolowski 2019).

The metal chelating ability of EDTA, ML-AgNPs, and *M. lucida* extract ranged from 23–92, 19–65, and 2.0–47%, respectively (Fig. 10), and the results revealed

Table 3 IC_{50} values of M. lucida and ML-AgNPs on free radicals

	IC_{50}		
	NO	OH^-	H_2O_2
ML-AgNPs	0.52 ± 0.09^b	1.68 ± 0.18^b	0.14 ± 0.0005^b
M. lucida extract	1.26 ± 0.025^a	1.93 ± 0.09^a	0.21 ± 0.004^a

Values with identical alphabets a and b are not significantly different at DMRT ($p < 0.05$)

Table 2 Antioxidant potential of *M. lucida* and ML-AgNPs

	TAC (AAE/g sample)	CUPRAC (mg TE/g sample)	Reductive potential
ML-AgNPs	229.89 ± 0.01^a	65.62 ± 1.07^a	2.07 ± 0.02^a
M. lucida extract	158.49 ± 0.001^b	28.63 ± 1.03^b	0.90 ± 0.005^b

Values with identical alphabets a and b are not significantly different at DMRT ($p < 0.05$)

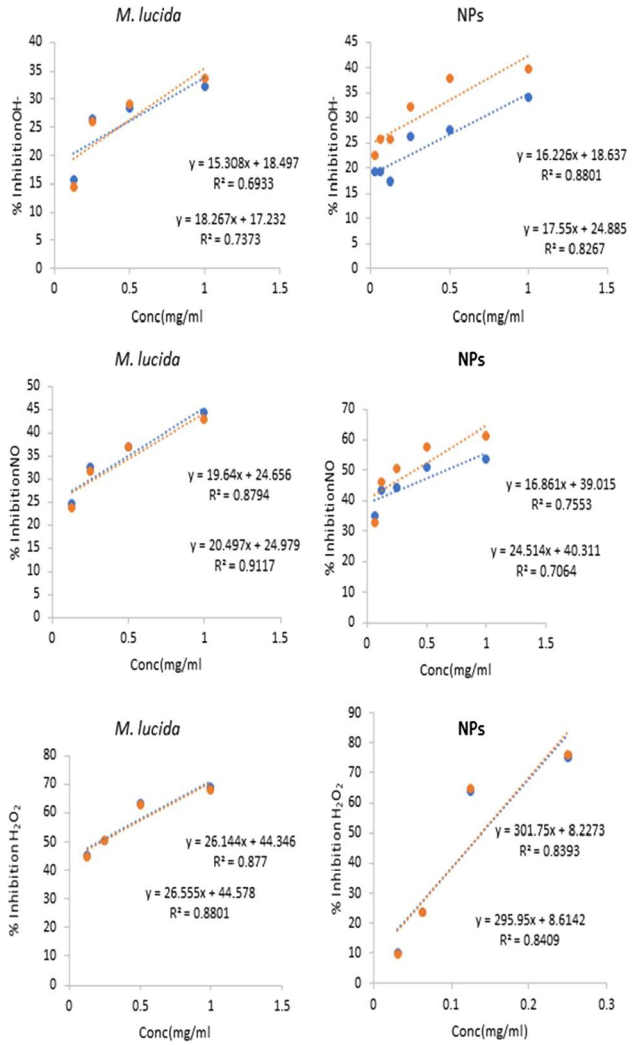

Fig. 9 Free radical scavenging potential of *M. lucida* extract and ML-AgNPs

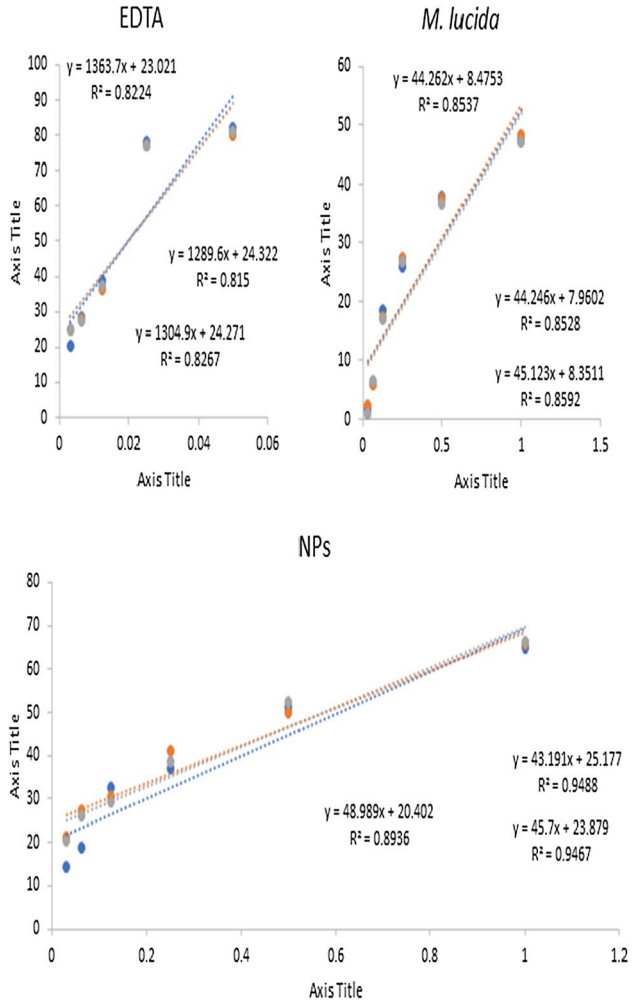

Fig. 10 Metal chelating abilities of *M. lucida* and ML-AgNPs

that ML-AgNPs had a stronger chelating impact than the crude plant extract and EDTA. In aqueous extracts of *M. lucida*, AgNPs of *M. lucida*, and EDTA, regression coefficient (R^2) values of 0.8592, 0.9488, and 0.8267 were observed, indicating that ML-AgNPs are capable of dispersing in solutions with high surface area to volume ratio while providing active sites for the interaction between the metal ions and the chelate ML-AgNPs. The metal chelating action intensified as the concentration of ML-AgNPs increased. When evaluated using two-way ANOVA, all of the values were found to be significant at $p < 0.05$, as shown in Table 3. Overall, the findings show that green-produced ML-AgNPs exhibit significant metal chelating activity toward metal ions (Fig. 10). The green synthesis of silver nanoparticles with *S. wightii* resulted in AgNPs with adequate antioxidant properties. Ponmani et al. (2020), obtained comparable results to those reported in this investigation.

Anti-microbial activity

Anti-microbial screening

The antimicrobial potency of both *M. lucida* extract and ML-AgNPs was examined against *E. coli*, *S. typhi*, *V. cholera*, *P. vulgaris*, *E. faecalis,* and *Citrobacter* using the disc diffusion method (Fig. 11). The results showed the extent of susceptibility of the examined organisms. The organisms showed varied zone of inhibition against the *M. lucida* extract and ML-AgNPs. The ML-AgNPs showed the maximum zone of inhibition of 43 nm against the *P. vulgaris* compared to 11 nm obtained for *M. lucida* extract (Table 4). The minimum inhibition of 16 and 9 nm was

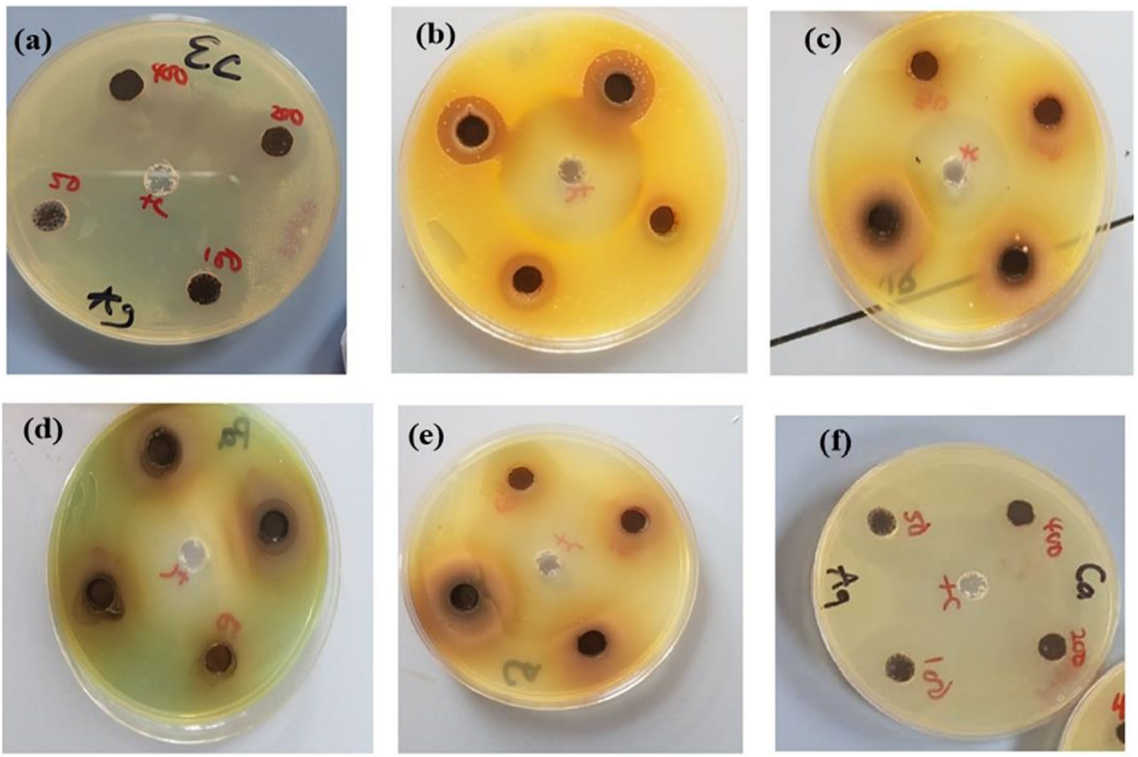

Fig. 11 Antimicrobial screening of **a** *E. coli* **b** *S. typhi* **c** *V. cholerae* **d** *P. vulgaris* **e** *E. faecalis* **f** *Citrobacter*

Table 4 The antibacterial potency and zone of inhibition of *M. lucida* extract and ML-AgNPs against bacteria

S/N	Bacteria	Zone of inhibition (nm)	
		M. lucida extract	ML-AgNPs
1	*E. coli*	10 ± 0.95	26 ± 0.10
2	*P. vulgaris*	11 ± 0.42	43 ± 0.64
3	*S. typhi*	13 ± 1.05	31 ± 0.59
4	*V. cholerae*	8 ± 1.53	29 ± 0.68
5	*E. faecalis*	10 ± 3.01	18 ± 1.12
6	*Citrobacter*	9 ± 1.48	16 ± 6.23

obtained for ML-AgNPs and *M. lucida* extract, respectively, against *Citrobacter.* Additionally, the high susceptibility of ML-AgNPs against these organisms indicated that the synthesized ML-AgNPs could be a valuable candidate for the treatment of infectious diseases especially as it has been reported that AgNPs have proved effective against SARS-CoV-2 or the new variant COVID-19 that have claimed over 1.8 million lives (Almanza-Reyes 2021). Thus, exploiting the use of readily available green plants for the synthesis of nanoparticles could create wealth and proffer solutions to problems ravaging mankind in the health sector.

Conclusions

In this study, ML-AgNPs were synthesized using the eco-friendly greener approach. The aqueous extract of the *M. lucida* was employed not only as the reducing but also as a capping agent and antioxidant. The color change, UV–vis adsorption and EDX confirm the reduction in Ag^{+} to Ag^{0}. The TEM showed that the ML-AgNPs' average particle size was 11 nm and was spherical. The FTIR results are in agreement with the total phenolic compound analysis. The ML-AgNPs are stable and have good antioxidant and antimicrobial activities. The green synthesized ML-AgNPs approach is quick, cost-effective, environmentally benign, non-toxic, and suited for large-scale manufacturing. However, more research is needed to show various biological properties (such as antifungal, antidiabetic, anti-inflammatory, and cytotoxic potential) as well as their mechanism of action.

Acknowledgements The authors acknowledge the contribution of Nwodo Anastasia and the entire members of the Nanotechnology Research Group of the Federal University of Lafia, Nigeria.

Declarations

Conflict of interest The authors declare no conflict of interest.

References

Abbiw DK (1990) Useful plants of Ghana: West African uses of wild and cultivated plants. Practical Action Publications, London, p 337

Agyare C, Obiri DD, Boakye YD, Osafo N (2013) Medicinal plant research in Africa. Pharmacology and chemistry anti-inflammatory and analgesic activities of African medicinal plants. Elsevier, Amsterdam, pp 725–752

Ajitha B, Ahn CW, Yadav PVK, Reddy YAK (2021) Silver nanoparticle embedded polymethacrylic acid/polyvinylpyrrolidone nanofibers for catalytic application. J Environ Chem Eng 9(5):106291

Akintelu SA, Olugbeko SC, Folorunso AS, Oyebamiji AK, Folorunso FA (2021) Potentials of phytosynthesized silver nanoparticles in biomedical fields: a review. Int Nano Lett 11:1–21

Aldosary SK, Abd El-Rahman SN (2019) Green synthesis and antibacterial properties of silver nanoparticles of lawsonia inermis, rhamnus frangula, camellia sinensis and thymus vulgaris extracts. J Pure Appl Microbiol 13(2):1279–1284

Almanza-Reyes H (2021) Evaluation of Silver Nanoparticles for the Prevention of SARS-CoV-2 Infection in Health Workers. In Vitro and in Vivo. PLoS ONE 16(8):1–14

Ansar S, Tabassum H, Aladwan NSM, Ali MN, Almaarik B, AlMahrouqi S, Abudawood M, Banu N, Alsubki R (2020) Eco friendly silver nanoparticles synthesis by Brassica oleracea and its antibacterial, anticancer and antioxidant properties. Sci Rep 10(18564):1–12. https://doi.org/10.1038/s41598-020-74371-8

Aref MS, Salem SS (2020) Bio-callus synthesis of silver nanoparticles, characterization, and antibacterial activities via *Cinnamomum camphora* callus culture. Biocatal Agric Biotechnol 27:101689

Contreras EQ (2012) Investigating the biological impacts of nanoengineered materials in Caenorhabditis elegans and in vitro. Rice University

Dada AO, Ojediran JO, Dada FE, Olalekan AP, Awakan OJ (2015) Green synthesis and characterization of silver nanoparticles using *Calotropis procera* extract. J Appl Chem Sci Int 8(4):137–143

Dhanapal R (2012) Nanotechnology engineering—a review. J Sci 2(1):13–15

Feng Y, Zhu Y, Wan J, Yang X, Firempong CK, Yu J, Xu X (2018) Enhanced oral bioavailability, reduced irritation and increased hypolipidemic activity of self-assembled capsaicin prodrug nanoparticles. Journal of Functional Foods 44:137–145

Flieger J, Franus W, Panek R, Szymańska-Chargot M, Flieger W, Flieger M, Kołodziej P (2021) Green synthesis of silver nanoparticles using natural extracts with proven antioxidant activity. Molecules 26(16):4986. https://doi.org/10.3390/molecules26164986

Green LC, Wagner DA, Glogowski J, Skipper PL, Wishnok JS, Tannenbaum SR (1982) Analysis of nitrate, nitrite, and [^{15}N] nitrate in biological fluids. Anal Biochem 126:131–138. https://doi.org/10.1016/0003-2697(82)90118-X

Gulcin I, Kufrevioglu OI, Oktay M, Buyukokuroglu ME (2004) Antioxidant, antimicrobial, antiulcer and analgesic activities of nettle (Urtica dioica L.). J Ethnopharmacol 90:205–215

Gutorova SV, Apyari VV, Kalinin VI, Furletov AA, Tolmacheva VV, Gorbunova MV, Dmitrienko SG (2021) Composable paper-based analytical devices for determination of flavonoids. Sens Actuators, B Chem 331:129398

Halliwell B, Gutteridge JM, Aruoma OI (1987) The deoxyribose method: a simple "test-tube" assay for determination of rate constants for reactions of hydroxyl radicals. Anal Biochem 165(1):215–219. https://doi.org/10.1016/0003-2697(87)90222-3 (**PMID: 3120621**)

Hamelian M, Mahdi M, Amisama A, Varmira K (2018) Green synthesis of silver nanoparticles using Thymus kotschyanus extract and evaluation of their antioxidant, antibacterial and cytotoxic effects. Appl Organometal Chem. https://doi.org/10.1002/aoc.4458

Hano C, Abbasi BH (2022) Plant-based green synthesis of nanoparticles: production, characterization, and applications. Biomolecules 12(31):4–9

Hedge S, Bera T, Roy A, Singh G, Ramachandrarao P, Dash D (2010) Characterization of enhanced antibacterial effects of novel silver nanoparticles. Nanotechnology 18:103–112. https://doi.org/10.1016/j.nano.2009.06.005

Jayaprakasha GK, Lingamallu JR, Kunnumpurath KS (2004) Antioxidant activities of flavidin in different in-vitro model system. Bioorg Med Chem 12:5141–5146

Jiang C, Bai Z, Yuan F, Ruan Z, Wang W (2022) A colorimetric sensor based on Glutathione-AgNPs as peroxidase mimetics for the sensitive detection of Thiamine (Vitamin B1). Spectrochim Acta Part A Mol Biomol Spectrosc 265:120348

Khan I, Saeed K, Khan I (2019) Nanoparticles: properties, applications and toxicities. Arab J Chem 12(7):908–931

Khan J, Chandra J, Xalxo R, Korram J, Satnami ML, Keshavkant S (2021) Amelioration of ageing associated alterations and oxidative inequity in seeds of Cicer arietinum by silver nanoparticles. J Plant Growth Regul 40(3):1341–1351

Khandel P, Shahi SK, Soni DK, Yadaw RK, Kanwar L (2018) Alpinia calcarata: potential source for the fabrication of bioactive silver nanoparticles. Nano Converg 5:37

Khanom R, Parveen S, Hasan M (2018) Antimicrobial activity of SnO2 nanoparticles against E. coli and S. aureus and conventional antibiotics. Am Sci Res J Eng Technol Sci 46(1):111–121

Konappa N, Udayashankar AC, Dhamodaran N, Krishnamurthy S, Jagannath S, Uzma F, Pradeep CK, De Britto S, Chowdappa S, Jogaiah S (2021) Ameliorated antibacterial and antioxidant properties by *Trichoderma harzianum* mediated green synthesis of silver nanoparticles. Biomolecules 11(535):15–16. https://doi.org/10.3390/biom11040535

Kumar V, Singh S, Srivastava B, Bhadouria R, Singh R (2019) Green synthesis of silver nanoparticles using leaf extract of Holoptelea integrifolia and preliminary investigation of its antioxidant anti-inflammatory antidiabetic and antibacterial activities. J Environ Chem Eng. https://doi.org/10.1016/j.jece.2019.103094

Labulo AH, Adesuji ET, Elemike EE, Onwuka JC, Bamgbose JT (2015) Green synthesis and growth kinetics of nanosilver under bio-diversified plant extracts influence. J Nanostruct Chem 5(1):85–94

Li R, Pan Y, Li N, Wang Q, Chen Y, Phisalaphong M, Chen H (2020) Antibacterial and cytotoxic activities of a green synthesized silver nanoparticles using corn silk aqueous extract. Colloids Surf, A 598:124827

Li J, Dai S, Qin R, Shi C, Ming J, Zeng X, Wen X, Zhuang R, Chen X, Guo Z, Zhang X (2021) Ligand engineering of titanium-oxo nanoclusters for Cerenkov radiation-reinforced photo/chemodynamic tumor therapy. ACS Appl Mater Interfaces 13(46):54727–54738. https://doi.org/10.1021/acsami.1c16213

Marcocci L, Maguire JJ, Droylefaix MT, Packer L (1994) The nitric oxide-scavenging properties of *Ginkgo biloba* extract EGb 761. Biochem Biophys Res Commun 201:748–755. https://doi.org/10.1006/bbrc.1994.1764

Matin S, Ahmad M, Swami BL, Ikram S (2017) Green synthesis of silver nanoparticles using *Azadirachta indica* aqueous leaf extract. J Radiat Res Appl Sci 9(1):1–7

Medina-Cruz S, Ahmad M, Swami BL, Ikram S (2020) Green synthesis of silver nanoparticles using *Azadirachta indica* aqueous leaf extract. J Radiat Res Appl Sci 9(1):1–7

Naikoo GA, Mustaqeem M, Hassan IU, Awan T, Arshad F, Salim H, Qurashi A (2021) Bioinspired and green synthesis of nanoparticles from plant extracts with antiviral and antimicrobial properties: a critical review. J Saudi Chem Soc 25:101304

Ndlovu N, Mayaya T, Muitire C, Munyengwa N (2020) Nanotechnology applications in crop production and food systems. Int J Plant Breed Crop Sci 7(1):603–613

Nityanada F, Kaushik P (2012) Green synthesis of silver nanoparticles through reduction with Solanum xanthocarpum L. berry extract: characterization antimicrobial and urease inhibitory activities against Helicobacter pylori. Int J Mol Sci 13(8):9923–9941

Ojemaye MO, Okoh SO, Okoh AI (2021) Silver nanoparticles (AgNPs) facilitated by plant parts of Crataegus ambigua Becker AK extracts and their antibacterial, antioxidant and antimalarial activities. Green Chem Lett Rev 14(1):51–61

Oyaizu M (1986) Studies on products of browning reaction prepared from glucosamine. Jpn J of Nutr 44:307–315

Palani R, Ayyasamy PM, Kathiravan R, Subashni B (2015) Rapid decolorization of synthetic melanoidin by bacterial extract and their mediated silver nanoparticles as support. J Appl Biol Biotechnol 3(02):6–11. https://doi.org/10.7324/jabb.2015.3202

Patil Shriniwas P, Kumbhar Subhash T (2017) Antioxidant, antibacterial and cytotoxic potential of silver nanoparticles synthesized using terpenes rich extract of Lantana camara L leaves. Biochem Biophys Rep 10:76–81

Ponmani J, Kanakarajan S, Selvaraj R, Kamalanathan A (2020) Antioxidant Properties of Green Synthesized Silver Nanoparticles from Sargassum wightii. Saudi J Med Pharm Sci 6(8):516–525

Rahimi-nasrabadi M, Pourmortazavi SM, Shandiz SA, Ahmadi F, Batooli H (2014) Green synthesis of silver nanoparticles using Eucalyptus leucoxylon leaves extract and evaluating the antioxidant activities of extract. Nat Prod Res 28(22):1964–1969. https://doi.org/10.1080/14786419.2014.918124

Raja S, Kumar A, Hashmi A, Khan Z (2017) Silver nanoparticles: preparation, characterization, and kinetics. Adv Mater Lett 2(3):188–194

Ranjitham AM, Suja R, Caroling G, Tiwari S (2013) In vitro evaluation of antioxidant, antimicrobial, anticancer activities and characterization of *Brassica oleracea*. var. Bortrytis. L synthesized silver nanoparticles. Int J Pharm Pharm Sci 5:239–251

Shoor SS, Lodise M (2006) Rapidsynthesis of Au, Ag, and bimetallic Au coree Ag shell nanoparticles using Neem (Azadirachta indica) leaf broth. Journal of Colloid and Interface Science 275(2):496

Singh N, Rajini PS (2004) Free radical scavenging activity of an aqueous extract of potato peel. Food Chem 85:611–616. https://doi.org/10.1016/j.foodchem.2003.07.003

Singh G, Rai M, Yadav A, Gade A (2013) Silver nanoparticles as a new generation of antimicrobials. Biotechnol Adv 27:76–83

Sytu MRC, Camacho DH (2018) Green synthesis of silver nanoparticles (AgNPs) from *Lenzites betulina* and the potential synergistic effect of AgNP and capping biomolecules in enhancing antioxidant activity. BioNanoScience 8:835–844

Tran L, Nunan L, Redman RM, Mohney LL, Pantoja CR, Fitzsimmons K, Lightner DV (2013) Determination of the infectious nature of the agent of acute hepatopancreatic necrosis syndrome affecting penaeid shrimp. Dis Aquat Org 105:45–55. https://doi.org/10.3354/dao02621

Ulewicz-Magulska B, Wesolowski M (2019) Total phenoliccontents and antioxidant potential of herbs used for medical and culinary purposes. In AGRIS 74(1):61–67

Verma A, Stellacci F (2010) Effect of surface properties on nanoparticle–cell interactions. Small 6(1):12–21

Wu P, Dai S, Chen G, Zao S, Xu Z, Fu M, Chen P, Chen Q, Jin X, Qiu Y, Yang S, Ye D (2020) Interfacial effects in hierarchically porous α-MnO_2/Mn_3O_4 heterostructures promote photocatalyic oxidation activity. App Catalysis: B 268:57. https://doi.org/10.1016/j.apcatb.2019.118418

Xu Y, Dai S, Li B, Xia Q, Li S, Peng W (2021) Protective strategy to boost the stability of animated graphene in fenton-like reactions. Environ Sci Technol 55(21):14828–14835. https://doi.org/10.1021/acs.est.1c03091

Zangeneh MM, Joshani Z, Zangeneh A, Miri E (2019) Green synthesis of silver nanoparticles using aqueous extract of Stachys lavandulifolia flower, and their cytotoxicity, antioxidant, antibacterial and cutaneous wound - healing properties. Appl Organometal Chem. https://doi.org/10.1002/aoc.5016

Zhao Y, Fan M, Zhou W, Li Y, Wang Y, Xiu Z, Gao B (2021) Speciation, controlling steps and pathways of silver release from the sludge generated from coagulation of wastewater spiked with silver nanoparticles. Chemosphere 282:131093